Available online at www.sciencedirect.com
SCIENCE DIRECT®

polymer

Polymer 47 (2006) 3028–3035

www.elsevier.com/locate/polymer

Viscosity of bulk free radical polymerizing systems under near-isothermal and non-isothermal conditions

Jitendra S. Sangwai, Deoki N. Saraf [1], Santosh K. Gupta *

Department of Chemical Engineering Indian Institute of Technology, Kanpur 2080 16, UP, India

Received 4 October 2005; received in revised form 14 February 2006; accepted 2 March 2006

Abstract

A viscometer-reactor assembly is used to generate data on the viscosity, $\eta(t)$, of an example polymerizing system exhibiting the Trommsdorff effect, namely, the bulk free radical polymerization of methyl methacrylate (MMA), at different temperature conditions [near-isothermal and non-isothermal (near-step increase and near-step decrease in temperature)] and at two different initiator, 2,2′-azoisobutyronitrile (AIBN), concentrations. Two types of cup and bob assemblies, viz., the Haake® SV-2 and the Haake® HV-DIN, have been used to measure $\eta(t)$ of the reaction mass, until reasonably high values of viscosity, well into the gel effect region. Only three sets of experimental data on $x_m(t)$, $M_w(t)$ and $\eta(t)$ under near-isothermal conditions, are used to develop general correlations for the viscosity. These tuned correlations predict the values of the viscosity for a whole variety of other experimental conditions, including non-isothermal cases, reflecting that the physics of the system is well represented by them. Hence, these correlations can be used for other systems after tuning their parameters. The feasibility of on-line soft sensing is demonstrated for a few cases.

Keywords: Bulk free radical polymerization; Rheokinetics; Soft sensor

1. Introduction

Several bulk free radical polymerizations, e.g. polymethyl methacrylate (PMMA), polystyrene (PS), copolymers, etc. exhibit the gel (Trommsdorff [1,2]), glass and cage effects. After the onset of the gel effect, the monomer conversion, x_m, and the weight average molecular weight, M_w, increase rapidly, leading to a dramatic increase of the viscosity, η, of the reaction mass. Good correlations for η are needed for such systems, not only because of their fundamental importance in rheology, but also for the proper design and operation of reactors. In addition, these correlations can provide the framework for studying reactive extrusions [3], as well as systems in which rapidly polymerizing liquids are flowing inside mold-cavities [4].

In contrast to the extensive amount of viscometric data and correlations available for non-reacting polymer solutions and melts, only some information is available for polymerizing systems. Some workers [5–7] have measured the viscosity as well as the monomer conversion and the average molecular weight of a few reacting systems simultaneously, using rheo-dilatometers in which the viscosity is estimated using different techniques (coaxial, capillary flow, ultrasound, etc.) as a function of time, *t*. Gonzalez-Romero and Macosko [8] studied the increase in viscosity during the rapid free radical copolymerization of styrene-dimethacrylate, a cross-linking system, using a specially designed cone and plate viscometer. Recently, Cioffi et al. [9] measured the viscosity of two polymerizing systems, styrene and *n*-butylmethacrylate, in a cone and plate rheometer and in a specifically designed helical barrel rheometer. They found the gel effect to reduce significantly at high shear rates (about 100 s^{-1}), thus providing a means to control this phenomenon. In their review of the rheokinetics of polymerizations [10], they indicate that most of the workers in this area have measured viscosities of solution polymerizations in an off-line manner and at early stages of polymerization, and not much information is available on bulk free radical polymerizations at high monomer conversions. Mankar et al. [11,12] carried out bulk polymerization of MMA in a specially designed viscometer-reactor assembly under near-isothermal conditions. They measured the viscosity and the temperature as a function of time and developed

---

* Corresponding author. Tel.: +91 512 259 7031/7127; fax: +91 512 259 0104.

E-mail address: skgupta@iitk.ac.in (S.K. Gupta).

[1] Presently at the University of Petroleum and Energy Studies, Dehradun 248007, India.

0032-3861/$ - see front matter © 2006 Elsevier Ltd. All rights reserved.
doi:10.1016/j.polymer.2006.03.007

Nomenclature

$A_{i,1}$, $A_{i,2}$	empirical kinetic parameters ($i=1$–4) (K^{-1}, –)
$B_{i,1}$, $B_{i,2}$	empirical kinetic parameters ($i=1$–4) (K^{-1}, –)
a, b, K'	empirical parameters in the viscosity correlation (Eq. (10))
C_{polym}	concentration of polymer (kg m^{-3})
d_0, d_1, d_2	empirical parameters in the viscosity correlation (Eq. (4))
J_i	empirical parameter in Eq. (9) ($i=1$–4; –, K, K^{-1}, K^{-2})
k_p, k_{tm}	rate constants for propagation and chain transfer to monomer in the presence of the gel and glass effects (m^3 kmol^{-1} s^{-1})
k_p^0, k_{tc}^0, k_{td}^0, k_{tm}^0	k_p, k_{tc}, k_{td}, k_{tm} in the absence of the gel or glass effects (m^3 kmol^{-1} s^{-1})
k_{po}^0, k_{tmo}^0	frequency factors for the intrinsic rate constants (s^{-1} or m^3 kmol^{-1} s^{-1})
M_w	weight average molecular weight [$\equiv(\mathrm{MW}_m)(\lambda_2+\mu_2)/(\lambda_1+\mu_1)$] (kg kmol^{-1})
MW_m	molecular weight of the monomer (kg kmol^{-1})
$T(t)$	temperature of the reaction mixture at time t (K or °C)
t	time (min)
$x_m(t)$	monomer conversion (molar) at time t [$\equiv 1-(M/M_0)$]

Greek letters

γ	shear rate (s^{-1})
η	viscosity of the reaction mass (Pa s)
η_{int}	intrinsic viscosity (kg^{-1} m^3)
η_{sol}	viscosity of the solvent (monomer) (Pa s)
μ_n	number average chain length at time t [$\equiv(\lambda_1+\mu_1)/(\lambda_0+\mu_0)$]
ρ_m, ρ_p	density of pure (liquid) monomer and polymer at temperature T (kg m^{-3})
τ	shear stress (Pa)
ϕ_m, ϕ_p	volume fractions of monomer and polymer in liquid at time t

a correlation relating η to x_m and M_w for different (isothermal) temperatures and initiator loadings, $[I]_0$. However, they were not too successful in providing generalized correlations, because of the lack of a good kinetic model and insufficient experimental data on $\eta(t)$ at different $T(t)$.

The thrust of this work is to carry out bulk free radical polymerizations of an example system, methyl methacrylate (MMA), in a viscometer-reactor assembly using 2,2′-azoisobutyronitrile (AIBN) as an initiator, and measure η, x_m and M_w as a function of time, t, well into the gel effect region, under different near-isothermal and non-isothermal temperature histories. The range of applicability of the earlier correlation of Mankar et al. [11,12] can then be extended, and more general correlations applicable to all initiator loadings and temperature histories can be developed. These correlations will also be useful for on-line soft sensing [determining the 'state' of the polymerizing system, i.e. x_m and M_w, using available data on $T(t)$ and $\eta(t)$], on-line model improvement and on-line optimal control, procedures being used in several industrial polymerizations but not documented too well in the open literature.

2. Measurement of viscosity

2.1. Experimental set-up

The experimental system used to generate data on the viscosity of polymerizing systems using the Haake® (Gebrueder Haake GmbH, Germany) SV-2 cup-and-bob assembly under a variety of temperature histories, has been described in our previous papers [13,14; Fig. 1]. This is not being repeated here. An additional cup-and-bob assembly, similar to the Haake® SV-2, is used in the present study. The details of this unit are shown in Fig. 1. The latter can measure much higher viscosities of up to 400,000 Pa s while the SV-2 can go only to about 35,000 Pa s (the bob

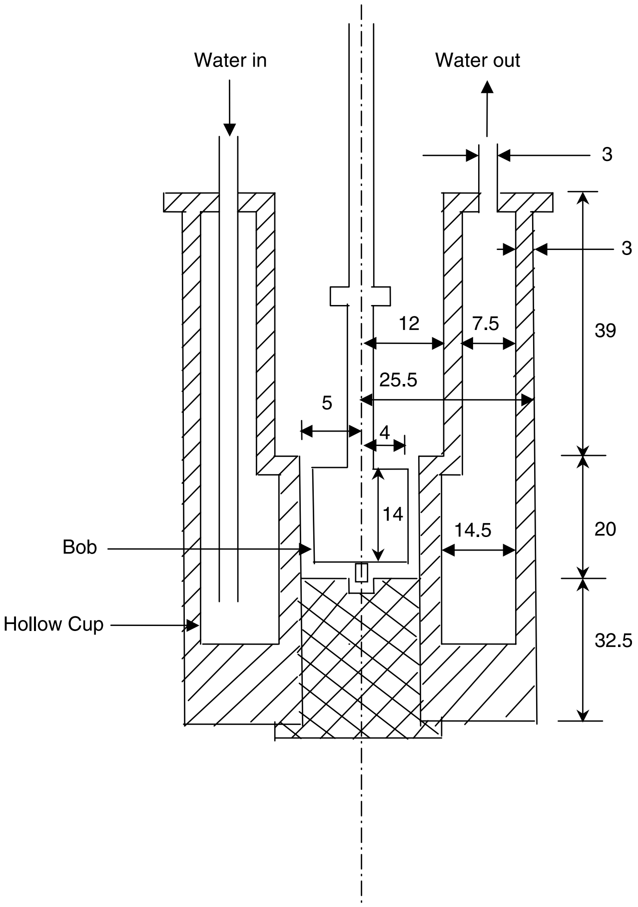

Fig. 1. Schematic diagram of the modified HVDIN cup-and-bob assembly. All dimensions are in mm (not to scale).

Table 1
Curve-fitted $T(t)$ for the various experimental runs in the HVDIN cup-and-bob assembly

Run no.	Experimental condition	$[I]_0$ (mol/m^3)	Pressure (kPa)	Fitted $T(t)$ in the HVDIN assembly[a]
1	NI50	15.48	100	$-0.235t^3+1.486t^2-1.474t+47.131$; $t<4.30$ 50; $t\geq 4.30$
2	NI50	25.8	100	$-0.211t^3+1.475t^2-1.531t+45.984$; $t<4.58$ 50; $t\geq 4.58$
3	NI60	15.48	100	$-0.235t^3+1.987t^2-1.228t+45.423$; $t<5.97$ 60; $t\geq 5.97$
4	NI60	25.8	100	$-0.190t^3+1.631t^2-0.506t+45.145$; $t<6.42$ 60; $t\geq 6.42$
5	NI70	15.48	250	$-0.194t^3+2.025t^2-1.372t+46.432$; $t<7.35$ 70; $t\geq 7.35$
6	NI70	25.8	250	$-0.214t^3+2.213t^2-1.810t+46.625$; $t<6.95$ 70; $t\geq 6.95$
7	NI80	15.48	350	$-0.068t^3+0.976t^2+0.429t+45.894$; $t<9.72$ 80; $t\geq 9.72$
8	NI80	25.8	350	$-0.066t^3+0.949t^2+0.512t+45.845$; $t<9.17$ 80; $t\geq 9.17$
9	SI50(60)70	15.48	250	$-0.305t^3+1.850t^2-1.703t+46.912$; $t<3.10$ 50; $3.10<t<60$ $-0.081(t-60)^3+0.769(t-60)^2+1.287(t-60)+49.851$; $60\leq t<67.70$ 70; $t\geq 67.70$
10	SI50(60)70	25.8	250	$-0.365t^3+2.060t^2-1.885t+46.940$; $t<3.85$ 50; $3.85<t<60$ $-0.075(t-60)^3+0.705(t-60)^2+1.455(t-60)+49.765$; $60\leq t<67.95$ 70; $t\geq 67.95$
11	SI50(120)70	15.48	250	$0.114t^3+0.455t^2-0.324t+47.031$; $t<2.50$ 50; $2.50<t<120$ $-0.125(t-120)^3+0.904(t-120)^2+2.366(t-120)+49.983$; $120\leq t<126.85$ 70; $t\geq 126.85$
12	SI50(120)70	25.8	250	$-0.387t^3+2.177t^2-2.038t+46.978$; $t<3.52$ 50; $3.52<t<120$ $-0.039(t-120)^3+0.441(t-120)^2+1.296(t-120)+49.886$; $120\leq t<127.75$ 70; $t\geq 127.75$
13	SI50(100)60	25.8	100	$-0.098t^3+0.588t^2+0.749t+44.047$; $t<3.82$ 50; $3.82<t<100$ $-0.088(t-100)^3+0.310(t-100)^2+2.759(t-100)+49.434$; $100\leq t<105.43$ 60; $t\geq 105.43$
14	SD70(20)50	15.48	250	$-0.089t^3+1.214t^2-1.108t+47.47$; $t<7.62$ 70; $7.62\leq t<20$ $-0.011(t-20)^3+0.497(t-20)^2-5.951(t-20)+71.709$; $20\leq t<27.20$ 50; $t\geq 27.20$
15	SD70(20)50	25.8	250	$-0.133t^3+1.501t^2-0.737t+46.825$; $t<7.82$ 70; $7.82\leq t<20$ $-0.002(t-20)^3+0.369(t-20)^2-5.635(t-20)+71.555$; $20\leq t<27.80$ 50; $t\geq 27.80$

[a] t in minute.

automatically stops rotating above these values so as to avoid damage to the measuring head).

2.2. Calibration of the cup-and-bob assemblies

The HVDIN cup-and-bob assembly is calibrated [11,12] prior to use. Standard viscosity test liquids [E6000 ($\eta=5$ Pa s) and E40000 ($\eta=43.3$ Pa s)], supplied by Gebrueder Haake GmbH, Germany are used for this purpose. The calibration obtained with relatively low viscosity test liquids is checked for higher viscosities by using two polymer melts: polystyrene ($M_w=220{,}986$ kg/kmol) at 180 °C, and poly methyl methacrylate ($M_w=125{,}314$ kg/kmol) at 210 °C, for the HVDIN assembly. The temperature of the polymer melt is controlled within ±0.7 °C using a Haake® TP500 temperature controller. The shear rate is kept low, at 0.06 s^{-1}. The results for these two systems are:

$$\eta_{\mathrm{PS}} = 48{,}750 \text{ Pa s} \qquad (1)$$

$$\eta_{\mathrm{PMMA}} = 102{,}200 \text{ Pa s}$$

which are within the experimental error of ±10% of the literature [15,16] values of 44,668 and 102,329 Pa s, respectively. This indicates that the calibration is trustworthy.

2.3. Experimental procedure

The detailed procedure for carrying out the polymerization, implementing the desired temperature history, $T(t)$, and measuring the viscosity, $\eta(t)$, is described by Mankar et al. [11] and is not repeated here. The pressure of the argon used to avoid formation of vapor bubbles in the viscometer gap is given in Table 1 for the several polymerization runs. In the case of the HVDIN cup-and-bob assembly, it was observed that the mixing of the reaction mixture as not satisfactory due to the small size of the bob. In order to improve this, the shear rate settings were kept at 50 s^{-1} in the beginning, 10 s^{-1} when the viscosity of the reaction mixture crossed 3–5 Pa s, 2 s^{-1} when the viscosity went beyond 15–30 Pa s, and finally, 0.1 s^{-1} after the viscosity increased to above 80–100 Pa s. The data obtained with this assembly superposes well with those reported earlier by Mankar et al. [11], indicating that the measured values of viscosity are trustworthy.

3. Results and discussion

3.1. Experimental

The viscosity of the polymerizing MMA system is measured using both the SV-2 and the HVDIN cup-and-bob assemblies at 15 different temperature histories, $T(t)$. These include

(a) Eight near-isothermal (NI) polymerizations in which the temperature is increased rapidly [13] from about 43 °C (the cup and bob assembly was preheated to this temperature) to the desired isothermal set-point value, T_{SP}, as soon as possible, and maintained at that point thereafter. During the initial heating period, very little polymerization takes place, and even though we refer to these runs as near-isothermal (to be technically correct), these are really isothermal polymerizations.

(b) Five (SI) cases in which the temperature is increased from about 45 °C to the desired initial T_{SP} as soon as possible, maintained at that point for some period, and then T_{SP} is increased by a desired amount (and the temperature maintained there once it attains that value). Run SI50(100)60 indicates a polymerization in which the temperature is increased to 50 °C in the beginning, maintained at that value for 100 min, and then T_{SP} is increased to 60 °C.

(c) Two (SD) cases in which the temperature is increased from about 45 °C to the desired initial T_{SP}, maintained at that point for some period, and then T_{SP} is decreased by a desired amount (and the temperature maintained there once it attains that value).

The temperatures are found to be controlled within ± 0.5 °C of the set-points for most of the duration except when the set-point is changed. The step change in the temperature is achieved within about 6–7 min [13].

Two initiator (AIBN) loadings of $[I]_0 = 15.48$ and 25.8 mol/m^3 are used. These are the same as those used by Balke and Hamielec [17] and Mankar et al. [11]. The temperature histories employed for all the runs for the two assemblies are similar in nature. The experimental temperature histories are curve-fitted to simple polynomials over different periods of time. These are given in Table 1 for all the cases for the HVDIN assembly ([13] gives these for the SV-2 assembly). The variation of the viscosity with time is measured for each of the cases. To the best of our knowledge, this is the first time that measurements of viscosities of bulk free radical polymerizations up to as high values as 400,000 Pa s have been reported in the open literature for a variety of non-isothermal cases. For all these runs, the polymerizing samples were stopped (quenched) in-between at different values of t and the corresponding values of x_m and M_w measured [13].

3.1.1. Experimental data at near-isothermal conditions

The experimental data on $x_m(t)$ and $M_w(t)$ for all the eight near-isothermal polymerizations taken with the HVDIN assembly were found to superpose well with earlier results taken either in small glass ampoules [17] or with the SV-2 assembly [11,13]. These results are not shown here for the sake of brevity. The superposition of these results for the several near-isothermal cases [11,13] with those of isothermal experimental conditions carried out by Balke and Hamielec [17] indicates that the present polymerizations are, indeed, isothermal even though they are termed near isothermal.

Figs. 2 and 3 show experimental results on $\eta(t)$ for $[I]_0 =$ 15.48 and 25.8 mol/m^3, respectively, for the eight near-isothermal cases. The SV-2 and HVDIN assemblies are not expected to give trustworthy values of η below about 5 and 10 Pa s, respectively, even though the values obtained using the two assemblies below these values match reasonably well for all $T(t)$. Since, the data using the two assemblies superpose quite well, only those taken with the HVDIN assembly are shown in these (and later) diagrams. It is observed that as the reaction temperature increases, the slope of the η vs. t curve increases. In addition, after the onset of the gel effect, the viscosity of the reaction mass increases very rapidly and we need to use smaller sampling times so as to get more data points in this period. The sampling time employed for the measurement of viscosity is 72 s at the beginning of the reaction and as the reaction progresses, the sampling time is gradually lowered to 5 s. It is found that the data shown in Figs. 2 and 3 for the NI50 case superpose quite well with those reported earlier by Mankar et al. [11]. However, our NI70 data on $\eta(t)$ for $[I]_0 = 25.8$ mol/m^3 for both the SV-2 and the HVDIN assemblies are not in accord with our earlier data [12] (latter are not shown). These workers had not checked $x_m(t)$ and $M_w(t)$ for the NI70 case against the data of Balke and Hamielec [17]. In contrast, we did measure [13] these quantities and found them to superpose well with those of Balke and Hamielec [17], who carried out the polymerization under isothermal conditions in small glass ampoules. This suggests that the present NI70 viscosity data is more trustworthy.

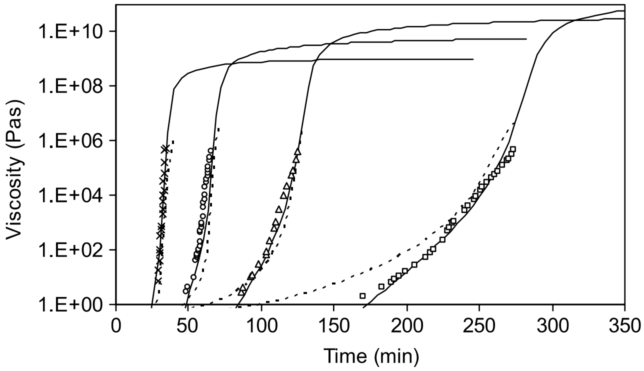

Fig. 2. Experimental data for $\eta(t)$ for near-isothermal conditions for $[I]_0 =$ 15.48 mol/m^3 (in absence of soft sensing and with the HVDIN assembly). □: NI50; △: NI60; ○: NI70; ×: NI80; – – –: predictions of Correlation 1 (Eq. (4)); —: predictions of Correlation 2 (Eq. (10)). Several data points have been deleted in all cases to improve clarity.

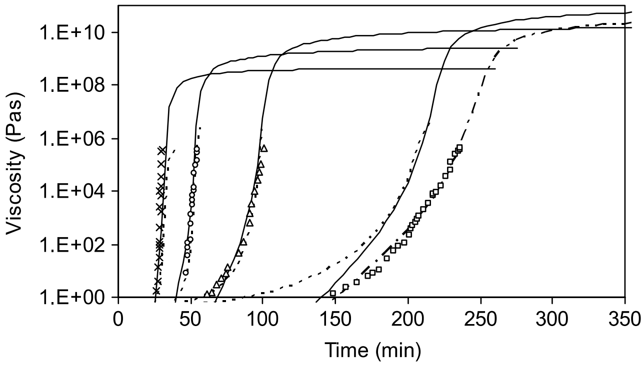

Fig. 3. Experimental data for $\eta(t)$ for near-isothermal conditions for $[I]_0 =$ 25.8 mol/m^3 (with the HVDIN assembly). □: NI50; △: NI60; ○: NI70; ×: NI80; – – –: predictions of Correlation 1 (Eq. (4)) without soft sensing; —: predictions of Correlation 2 (Eq. (10)) without soft sensing. — — —: predictions of Correlation 2 with soft sensing. Other details are as in Fig. 2.

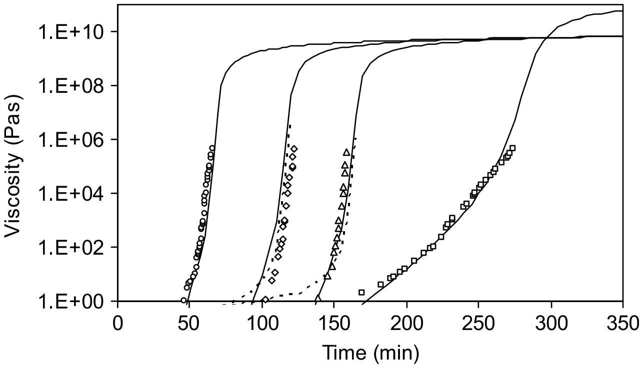

Fig. 4. Experimental data for $\eta(t)$ for non-isothermal conditions for $[I]_0 = 15.48\ \mathrm{mol/m^3}$ (with the HVDIN assembly and without soft sensing). ◇: SI50(60)70; △: SI50(120)70. Results for □: NI50 and ○: NI70 also shown for comparison. – – –: predictions of Correlation 1 (Eq. (4)); —: predictions of Correlation 2 (Eq. (10)). Other details are as in Fig. 2.

3.1.2. Experimental data under non-isothermal conditions

Figs. 4–8 show data on $\eta(t)$ for the non-isothermal cases described in Table 1 (along with results for some NI cases for comparison). The slope of the η vs. t curves for the SI runs approaches those for the higher temperature NI runs, while those for the SD cases approach those for the lower temperature NI runs. Corresponding data for $x_m(t)$ and $M_w(t)$ for these cases are available in Ref. [13].

3.2. Modeling

3.2.1. Kinetics of polymerization

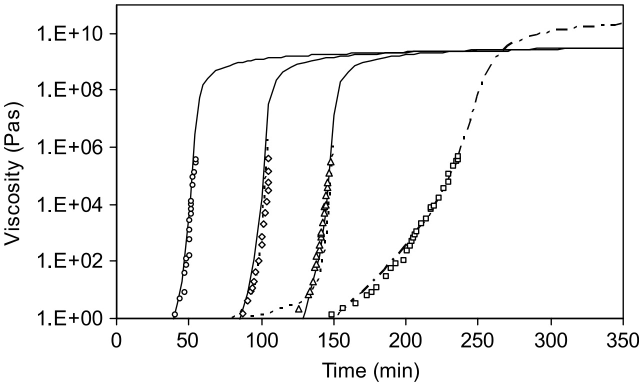

Fig. 5. Experimental data for $\eta(t)$ for non-isothermal conditions for $[I]_0 = 25.8\ \mathrm{mol/m^3}$ (with the HVDIN assembly). ◇: SI50(60)70; △: SI50(120)70. Results for □: NI50 and ○: NI70 also shown for comparison. – – –: predictions of Correlation 1 (Eq. (4)) without soft sensing; —: predictions of Correlation 2 (Eq. (10)) without soft sensing; — — — –: predictions of Correlation 2 (Eq. (10)) with soft sensing for NI50. Other details are as in Fig. 2.

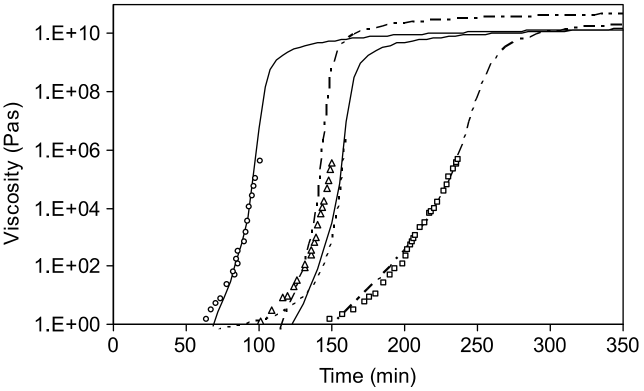

Fig. 6. Experimental data for $\eta(t)$ for non-isothermal conditions for $[I]_0 = 25.8\ \mathrm{mol/m^3}$ (with the HVDIN assembly). △: SI50(100)60. Results for □: NI50 and ○: NI60 also shown for comparison. – – –: predictions of Correlation 1 (Eq. (4)) without soft sensing; —: predictions of Correlation 2 (Eq. (10)) without soft sensing; — — —: predictions of Correlation 2 (Eq. (10)) with soft sensing for SI50(100)60 and NI50. Other details are as in Fig. 2.

Correlations for $\eta(t)$ for polymerizing systems require values of $x_m(t)$ and $M_w(t)$ for any temperature history. Hence, good kinetic models that can predict these are required. The latter are described in our earlier paper [13] but a short summary (and some further extensions) is presented here. The kinetic scheme for bulk free radical polymerization of MMA is given in Ref. [13]. It incorporates chain transfer to monomer (rate constant, k_{tm}) as well as termination by both disproportionation (k_{td}) and combination (k_{tc}). In that study, both k_{tm} and k_{tc} were assumed to be zero. We had proposed [13] the following simple extension of the model of Curteanu and Bulacovschi [18]:

$$k_{td} = k_{td}^0 \exp\left(A_1 + A_2 x_m + A_3 x_m^2 + A_4 x_m^3\right) \tag{2a}$$

$$k_p = k_p^0 \exp\left(B_1 + B_2 x_m + B_3 x_m^2 + B_4 x_m^3\right) \tag{2b}$$

$$A_i = A_{i1}(T - 273.15) + A_{i2}; \quad i = 1,2,3,4 \tag{2c}$$

$$B_i = B_{i1}(T - 273.15) + B_{i2}; \quad i = 1,2,3,4 \tag{2d}$$

This equation represents an empirical extension of the free-volume model of Hui and Hamielec [19] and, hence, has some molecular basis. Eq. (2), along with the set of mass balance and moment equations [13], has been found to work satisfactorily [13] for a variety of polymerizations, both isothermal and non-isothermal. Several workers [20–24] have, indeed, incorporated both k_{tc} and k_{tm} in their models, and we extend our previous [13] model to do the same. We obtain the following

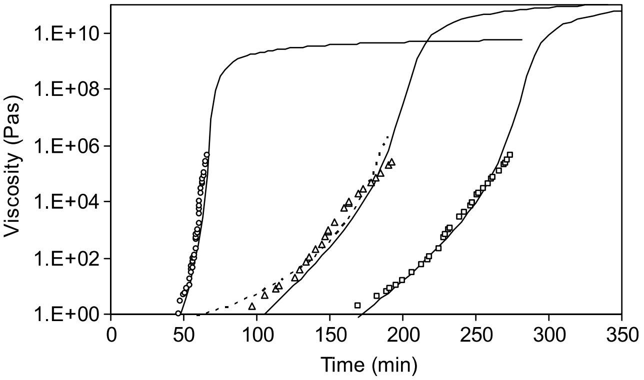

Fig. 7. Experimental data for $\eta(t)$ for non-isothermal conditions for $[I]_0 = 15.48\ \mathrm{mol/m^3}$ (with the HVDIN assembly and without soft sensing). △: SD70(20)50. Results for □: NI50 and ○: NI70 also shown for comparison. – – –: predictions of Correlation 1 (Eq. (4)); —: predictions of Correlation 2 (Eq. (10)). Other details are as in Fig. 2.

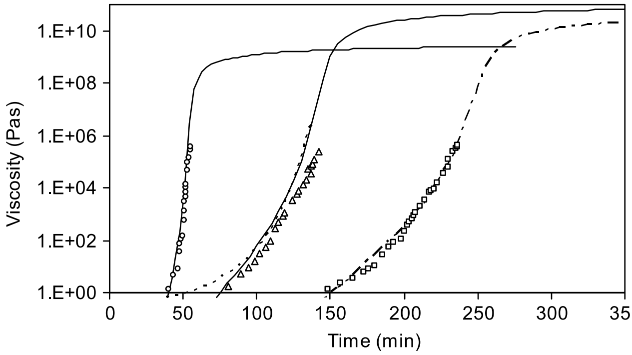

Fig. 8. Experimental data for $\eta(t)$ for non-isothermal conditions for $[I]_0=25.8$ mol/m^3 (with the HVDIN assembly). △: SD70(20)50. Results for □: NI50 and ○: NI70 also shown for comparison. – – –: predictions of Correlation 1 (Eq. (4)) without soft sensing; —: predictions of Correlation 2 (Eq. (10)) without soft sensing; — — —: predictions of Correlation 2 (Eq. (10)) with soft sensing for NI50. Other details are as in Fig. 2.

equation for termination by combination:

$$\frac{k_{\mathrm{tc}}}{k_{\mathrm{tc}}^0}=\frac{k_{\mathrm{td}}}{k_{\mathrm{td}}^0} \tag{3}$$

using the development of Chiu et al. [25]. A similar approach was used earlier to develop an expression [13] for k_{tm} to give $k_{\mathrm{tm}}/k_{\mathrm{tm}}^0=k_{\mathrm{p}}/k_{\mathrm{p}}^0$. Eqs. (2) and (3) and that for k_{tm} [13] {along with the values: $k_{\mathrm{td}}^0+k_{\mathrm{tc}}^0=9.800\times10^7\ \exp(-2.937\times10^3/RT)$, $(k_{\mathrm{tc}}^0/k_{\mathrm{td}}^0)=3.956\times10^{-4}\ \exp(17.1126\times10^3/RT)$ and $k_{\mathrm{tm}}^0=4.66\times10^9\exp(-74.28\times10^3/RT)$ [20]}, can be used with the set of mass balance and moment equations [26,27] to study the progress of polymerization under almost any experimental condition, i.e. $T(t)$ and $[I](t)$. The values of the 16 model parameters in Eq. (2) are tuned using the same procedure as described in Ref. [13]. It is observed that the tuned values of the model parameters with both k_{tc} and k_{tm} incorporated, are almost identical to those with only k_{tm} included (the parameters of the latter are given in Ref. [13]) and are used in this study henceforth.

3.2.2. Viscosity

Several workers [26,28] have suggested the use of the Lyons–Tobolsky equation [29] for modeling the viscosity of polymerizing systems. Gonzalez-Romero and Macosko [8] considered the viscosity increase during polymerization as a function of only x_{m} and T, and did not take into account its dependence on M_{w}. Mankar et al. [11] used an extension of the Martin equation [30]. Yet another correlation has been suggested by Malkin and Kulchikhin [5] and Malkin [6]. More recently, Song et al. [31] presented a simple model for the viscosity of multi-component liquids containing polymers. Any of these can be ‘tuned’ using experimental data to obtain suitable models. We have selected two of the several correlations available, namely the extended Martin equation and the correlation of Malkin and coworkers. As was done for the kinetic model, only some of the experimental data on $\eta(t)$ is used to ‘tune’ the parameters of the correlations for the viscosity, and then the model predictions are tested against the remaining data to see if the agreement with experimental results is good. The values of $x_{\mathrm{m}}(t)$ and $M_{\mathrm{w}}(t)$ for a specified $T(t)$ are obtained from the kinetic model, and used in the two correlations for $\eta(t)$.

The first model studied [11,30] is given by

Correlation 1:.

$$\eta=\eta_{\mathrm{sol}}[1+\eta_{\mathrm{int}}C_{\mathrm{polym}}\exp\{d_0+d_1(\eta_{\mathrm{int}}C_{\mathrm{polym}})+d_2(\eta_{\mathrm{int}}C_{\mathrm{polym}})^2\}] \tag{4}$$

where d_0–d_2 are constants to be fitted to data, and are independent of $T(t)$. In Eq. (4), η_{int} is the intrinsic viscosity, given for the MMA–PMMA system by [32]

$$\eta_{\mathrm{int}}(\mathrm{m}^3/\mathrm{kg})=5.2\times10^{-4}M_{\mathrm{w}}^{0.76}\quad(\text{for } M_{\mathrm{w}}\geq35{,}000\ \mathrm{kg/kmol}) \tag{5}$$

The above Mark–Houwink equation is for the PMMA–benzene system at 30 °C. However, this equation is actually used in Eq. (4) as one for M_{w}, and it does not matter if the temperature of the reaction mass is actually different from 30 °C, or if a different solvent is used. In Eq. (4), C_{polym} is the concentration of the polymer in the reaction mass at time, t, and is given by

$$C_{\mathrm{polym}}=(1-\phi_{\mathrm{m}})\rho_{\mathrm{p}} \tag{6}$$

where ϕ_{m} is the volume fraction of the monomer, and ρ_{p} is the density of the pure polymer. ϕ_{m}, in turn, can be related to the monomer conversion by

$$\phi_{\mathrm{m}}=\frac{(1-x_{\mathrm{m}})/\rho_{\mathrm{m}}}{(1-x_{\mathrm{m}})/\rho_{\mathrm{m}}+x_{\mathrm{m}}/\rho_{\mathrm{p}}} \tag{7}$$

In Eq. (7), ρ_{m} is the density of the pure monomer. The densities, ρ_{m} and ρ_{p}, are given by [20]

$$\rho_{\mathrm{m}}=966.5-1.1(T-273.15) \tag{8a}$$

$$\rho_{\mathrm{p}}=1200\ \mathrm{kg\ m}^{-3} \tag{8b}$$

Ref. [33] gives the viscosity, η_{sol}, of the solvent (pure monomer) as

$$\log_{10}\eta_{\mathrm{sol}}=J_1+J_2/T+J_3T+J_4T^2 \tag{9}$$

where J_1–J_4 are constants. The values of the various parameters used in the above correlation are available elsewhere [11].

The second correlation used in the present study is [5,6]:

Correlation 2:.

$$\eta=KX_{\mathrm{m}}^aM_{\mathrm{w}}^b \tag{10a}$$

$$\log_{10}\eta=K'+a\log_{10}X_{\mathrm{m}}+b\log_{10}M_{\mathrm{w}} \tag{10b}$$

where η has units of Pa s, and M_{w} has units of kg/kmol. In Eq. (10), X_{m} ($\equiv100x_{\mathrm{m}}$) is the percentage conversion of the monomer, and K', a, and b are constants (independent of temperature). This correlation has been used to study several polymerizations [34–36] as well as for explaining [3] phase separation during polymerization.

It may be emphasized here that Correlation 1 involves only a small explicit dependence on the temperature (through

ρ_m and η_{sol}) while Correlation 2 has no such (explicit) dependence. The effect of temperature enters primarily (and indirectly) through $x_m(t)$ and $M_w(t)$, which depend significantly on $T(t)$.

Mankar et al. [11,12] obtained individual sets of values of the three parameters d_0, d_1, d_2, in Eq. (4) using their data [11,12] on $\eta(t)$ for the NI50, NI60, and NI70 cases. It has already been pointed out earlier that their data on $\eta(t)$ for the NI70 run, for $[I]_0 = 25.8$ mol/m^3, is possibly in error. In fact, their values for the constants in Eq. (4) differ significantly for this particular case (while those obtained for the NI50 and NI60 runs for both $[I]_0s$ seem similar; this is one more reason why we believe that experimental data reported earlier [12] for NI70 may be in error).

In this work, we have tuned the parameters, d_0, d_1 and d_2, in Eq. (4) and K' in Eq. (10) (we have fixed $a = 12.8$ and $b = 3.4$ [5]) using only three sets of experimental data on $\eta(t)$. The data used for tuning are: NI50 for $[I]_0 = 15.48$ mol/m^3, and NI60 at both $[I]_0 = 15.48$ and 25.8 mol/m^3. Only a single, common set of values of the parameters is obtained. A code for simple genetic algorithm, SGA [37], is used for this. The tuning is done by minimizing the normalized sum of square errors, E, between the experimental data on $\eta(t)$ and the model-predicted values:

$$\text{Min } E(d_0, d_1, d_2; K') = \sum_{i=1}^{n_x} \left[\left(\frac{\eta_{mod}(t_i) - \eta_{exp}(t_i)}{\eta_{mod}(t_i)} \right)^2 \right] \tag{11}$$

In Eq. (11), subscripts, mod and exp, represent the model-predicted and corresponding experimental values, respectively, and n_x is the total number of data points available for $\eta(t)$. Table 2 gives the final values of the parameters obtained for the two correlations. This table also gives the values of the computational parameters used in the SGA code.

The predictions of the two correlations for $\eta(t)$ for all the NI runs (including those not used for tuning the parameters), are shown by dotted and continuous curves, respectively, in Figs. 2 and 3. Figs. 4–8 show the model-predictions of the viscosity for all the non-isothermal experimental conditions. It is observed from these figures that the predictions of the two correlations for the viscosity are quite similar, and match quite well with experimental data. The good agreement of the model predictions with experimental data even for systems not used for tuning (including those under non-isothermal conditions) indicates that either of the two models is quite good and general, and reflects the fact that they represent the physics of the problem well. Hence, we believe that these models (for η as well as x_m and M_w) are quite general, and can be used for other polymer systems as well, provided the parameters are tuned using some experimental data on $x_m(t)$, $M_w(t)$ and $\eta(t)$ for a specified $T(t)$ for the system of interest.

Table 2
Final values of the parameters of Eqs. (4) and (10), as well as the values and bounds used in SGA [37]

Computational parameters	
No. of parameters, n	Three for Eq. (4), and one for Eq. 10
Population size, N_p	50
Probability of crossover, P_c	0.9
Probability of mutation, P_m	0.003
Length of chromosome, l_{str}	15

Bounds

Tuning parameter	Lower bound	Upper bound	Final value
d_0, Eq. (4)	1.222	1.422	1.318
d_1, Eq. (4)	1.000×10^{-1}	2.000×10^{-1}	1.966×10^{-1}
d_2, Eq. (4)	-5.500×10^{-4}	-6.500×10^{-4}	-5.535×10^{-4}
K', Eq. (10)	-3.545×10^{1}	-3.945×10^{1}	-3.640×10^{1}

The sensitivity of the model to variations in the parameters of the two correlations is now studied. It is observed that Correlation 1 is less sensitive to changes in the values of the model parameters than Correlation 2. A change in the value of d_0 of ±2% around its tuned value gives about a ±10% change in $\eta(t)$. A similar result is observed for d_1. However, a change in d_2 by about ±10% around the tuned value changes $\eta(t)$ by only about ±4%. In contrast, Correlation 2 is found to be quite sensitive to changes in K': a ±2% in K' around its tuned value leads to almost a ±400% change in viscosity.

It may be mentioned that the predictions of Correlation 1 (Eq. (4)) are good only for values of viscosity below about 400,000 Pa s, the value used for tuning. Beyond this point, Correlation 1 shows a decrease in the value of the viscosity, which suggests the failure of this equation beyond this stage. This limitation should be kept in mind. In contrast, Correlation 2 (Eq. (10)) predicts increasing viscosities even after this point, and so can be used for the entire course of reaction. This advantage of Correlation 2 somewhat balances its disadvantages associated with its sensitivity.

3.3. On-line tuning

It is observed from Fig. 3 that the model predictions for both the correlations do not agree as well with experimental data for the NI50 case for $[I]_0 = 25.8$ mol/m^3, as they do for several other cases. Fig. 4 of Ref. [13] shows that the prediction of the kinetic model is also not satisfactory for this case. The poor fit of the viscosity correlations could possibly be attributed to the poor fit of the kinetic model for this case. If this is indeed so, the predictions could be improved using ‘soft sensing’, i.e. on-line re-tuning of some of the kinetic parameters using experimental data on $T(t)$ and $\eta(t)$ [and not $x_m(t)$ or $M_w(t)$, which cannot be measured on-line], as available at any time. After a few trials, it was found that only eight of the kinetic parameters, namely, A_{11}, A_{12}, A_{21}, A_{22}, B_{11}, B_{12}, B_{21}, and B_{22}, needed to be re-tuned. This procedure can actually be carried out several times so as to adapt the model continuously. However, we only illustrate the feasibility of re-tuning here. We use the entire set of data on $T(t)$ and $\eta(t)$ to re-tune (only once) the kinetic parameters. SGA is used for this purpose. The new parameters are given in Table 3, along with the values of the computational parameters used. The re-tuned model shows a remarkable improvement of the agreement for both the correlations, as shown in Fig. 3 (the predictions of the two re-tuned models are indistinguishable). In fact, the agreement

Table 3
Re-tuned values of some of the kinetic parameters (Eq. (2)) along with values of the computational parameters used in SGA [37]

Computational parameters	
No. of parameters, n	8
Population size, N_p	50
Probability of crossover, P_c	0.9
Probability of mutation, P_m	0.003
Length of chromosome, l_{str}	15

Bounds

Tuning parameter	Lower bound	Upper bound	Re-tuned values, NI50	Re-tuned values, SI50(100)60
A_{11}, K^{-1}	-2.690×10^{-2}	-0.79×10^{-2}	-1.364×10^{-2}	-0.950×10^{-2}
A_{12}	6.521×10^{-1}	9.781×10^{-1}	6.555×10^{-1}	7.0406×10^{-1}
A_{21}, K^{-1}	-3.036×10^{-1}	-2.024×10^{-1}	-2.092×10^{-1}	-2.998×10^{-1}
A_{22}	7.540	10.311	9.622	9.581
B_{11}, K^{-1}	-5.300×10^{-3}	-3.900×10^{-3}	-2.509×10^{-3}	-4.078×10^{-3}
B_{12}	9.690×10^{-2}	1.400×10^{-1}	9.017×10^{-2}	9.774×10^{-2}
B_{21}, K^{-1}	-3.138×10^{-1}	-2.225×10^{-1}	-2.142×10^{-1}	-2.726×10^{-1}
B_{22}	7.571	11.357	6.379	10.379

of $x_m(t)$ and $M_w(t)$ also improves significantly (results not shown). A similar improvement is observed for the case of the SI50(100)60 run with $[I]_0=25.8$ mol/m^3 (Fig. 6 and Table 3). These simple examples indicate the possibility of continuous soft sensing and model update. Such procedures are being carried out in industry for a variety of polymerizations, but very little documentation is available in the open literature.

4. Conclusions

Experimental data are generated for the viscosity of bulk free radical polymerization of MMA under a variety of temperature histories, isothermal as well as non-isothermal. Two correlations for the viscosity are developed and the model parameters are tuned using only three sets of near-isothermal data. The predictions of these tuned models are in good accord with other sets of experimental data, particularly under non-isothermal conditions, indicating that these models reflect the physics of the situation quite well, and so should be applicable to other systems too (after tuning using appropriate experimental data). The agreement of the model with a considerable amount of experimental results, particularly under non-isothermal conditions, provides a stringent test of the correlations. The feasibility of viscosity-based soft sensors for on-line state estimation and model update, is discussed.

Acknowledgements

Thanks are due to Mr Shrikant A. Bhat for his help with computer simulations, and to Mr J. S. Virdi for help in modifying the viscometer-reactor assembly. Financial supports from the Department of Science and Technology, [through grants III-5(13)/2001-ET and SR/S3/CE/46/2005-SERC-Engg] and the Ministry of Human Resource Development [through grant F.26-11/2004.TS.V, dated March 31, 2005], Government of India, New Delhi, are gratefully acknowledged.

References

[1] Trommsdorff VE, Köhle H, Lagally P. Makromol Chem 1947;1:169–98.
[2] Norrish RGW, Smith RR. Nature 1942;150:336–7.
[3] Janssen LPBM. Polym Eng Sci 1998;38:2010–9.
[4] Polushkin EY, Polushkina OM, Malkin AYa, Kulichikhin VG, Michaeli W, Kleba I, et al. Polym Eng Sci 2002;42:846–58.
[5] Malkin AYa, Kulchikhin SG. Polymer 1984;25:778–84.
[6] Malkin AYa. Polym Eng Sci 1980;20:1035–44.
[7] Kumar A, Gupta SK, Mohan R. Eur Polym J 1980;16:7–10.
[8] Gonzalez-Romero VM, Macosko CW. J Rheol 1985;29:259–72.
[9] Cioffi M, Hoffmann AC, Janssen LPBM. Chem Eng Sci 2001;56:911–5.
[10] Cioffi M, Ganzeveld KJ, Hoffmann AC, Janssen LPBM. Polym Eng Sci 2002;42:2383–92.
[11] Mankar RB, Saraf DN, Gupta SK. Ind Eng Chem Res 1998;37:2436–45.
[12] Mankar RB, Gupta SK, Saraf DN. J Appl Polym Sci 1999;73:2309–26.
[13] Sangwai JS, Bhat SA, Gupta S, Saraf DN, Gupta SK. Polymer 2005;46:11451–62.
[14] Mankar RB, Saraf DN, Gupta SK. J Appl Polym Sci 2002;85:2350–60.
[15] Hieber CA, Chiang HH. Rheol Acta 1989;28:321–32.
[16] Casale A, Moroni A, Civardi E. Die Angew Makromol Chem 1976;53:1–18.
[17] Balke ST, Hamielec AE. J Appl Polym Sci 1973;17:905–49.
[18] Curteanu S, Bulacovschi V. J Appl Polym Sci 1999;74:2561–70.
[19] Hui AW, Hamielec AE. J Appl Polym Sci 1972;16:749–69.
[20] Baillagou PE, Soong DS. Chem Eng Sci 1985;40:87–104.
[21] Achilias DS, Kiparissides C. J Appl Polym Sci 1988;35:1303–23.
[22] Konstadinidis K, Achilias DS, Kiparissides C. Polymer 1992;33:5019–31.
[23] Verros GD, Latsos T, Achilias DS. Polymer 2005;46:539–52.
[24] Allcock HR, Lampe FW. Contemporary polymer chemistry. 2nd ed. Englewood Cliffs, NJ: Prentice Hall; 1981.
[25] Chiu WY, Carratt GM, Soong DS. Macromolecules 1983;16:348–57.
[26] Seth V, Gupta SK. J Polym Eng 1995;15:283–326.
[27] Ray AB, Saraf DN, Gupta SK. Polym Eng Sci 1995;35:1290–9.
[28] Curteanu S, Bulacovschi V. Chem Ind 2004;58:393–400.
[29] Lyons PF, Tobolsky AV. Polym Eng Sci 1970;(10):1–3.
[30] Davis WE, Elliott JH. Flow properties. In: Ott E, Spurlin H, Grafflin MW, editors. High polymers. Cellulose and cellulose derivatives, part III, vol. 5. NY: Interscience; 1955. p. 1203–46.
[31] Song Y, Mathias PM, Tremblay D, Chen CC. Ind Eng Chem Res 2003;42:2415–22.
[32] Cohn-Ginsberg E, Fox TG, Mason HF. Polymer 1962;3:97–109.
[33] Yaws CL. Handbook of viscosity, vol. 2. Houston, TX: Gulf; 1995.
[34] Cioffi M, Hoffmann AC, Janssen LPBM. Nonlinear analysis 2001;47:897–906.
[35] Otterbach P, Lennarz K, Bargon J. Macromol Chem Phy 1994;195:3929–35.
[36] Kulichikhin SG, Malkin AYa, Polushkina OM, Kulichikhin VG. Polym Eng Sci 1997;37:1331–8.
[37] Goldberg DE. Genetic algorithms in search, optimization and machine learning. Reading, MA: Addison-Wesley; 1989.